Kinetics of environmental stress cracking in high density polyethylene

R. A. Bubeck
The Dow Chemical Company, Plastics Department R and D, 433A building, Midland MI 48640, USA
(*Received* 31 *March* 1980)

The observation of environmental stress crack (*ESC*) growth in high density polyethylene (HDPE) in a 10% Igepal CO-630 solution is reported using double-edge-notched specimens, which allow a fracture mechanics approach. Below the initial stress intensity factor K_I value of 0.4 MPa $m^{1/2}$, the cracking process consisted of both an incubation time for cracking, t_d, and a crack growth stage. The incubation time is stress dependent (decreasing with increasing stress), while the crack growth exhibits a root time ($t^{1/2}$) dependence and is relatively stress independent. The incubation time is the time necessary to generate a dry void craze structure sufficient to allow the PE to absorb the aggressive liquid. As a consequence of the liquid transport in the craze structure, the crack growth is believed to be controlled by the velocity of the liquid entering the void/fibril structure where capillary pressure is the driving force. The incubation times were determined to be more significant than the actual average crack growth rates for the PE samples tested. Injection moulding orientation increases the average crack growth rate without significantly changing the incubation time.

INTRODUCTION

A commercial limitation of polyethylene is the tendency of various resins to undergo environmental stress cracking (*ESC*) in contact with liquids such as detergents[1]. Some polyethylenes undergo *ESC* in a liquid as seemingly innocuous as water[2]. The mechanism of *ESC* in polyethylene first involves the formation of a dry pore/craze structure formed under stress. The pore/craze structure allows the aggressive liquid agent to enter the material, where capillary pressure is the driving force. The environmental stress crack discussed here consists of load-bearing bridging fibrils with pore structure at the tip, similar to crazes found in glassy polymers. The polyethylene in contact with the aggressive agent, is plasticized[3,4] by the aggressive agent, and fibrillates. The fibrils break down under load to form a crack. Elements of this description are substantiated in this paper.

EXPERIMENTAL

Marshall, Williams and coworkers[5,6] have applied fracture mechanics and the concept of the stress intensity parameter K_I as the controlling stress parameter for the study of environmental stress cracking kinetics. The test involves applying a constant stress σ to a specimen with a known flaw length (a razor slit) as in *Figure 1*. The precise polyaxial stress state at any point in the vicinity of the slit or precrack is defined by the stress intensity parameter K_I. The stresses of an elastic field of a crack can be mapped by the relations, as reviewed by Hayes[7]. For axial tensile loading of a single-edge-notch specimen or a double-edge-notch specimen, the stress intensity factor K_I is expressed as:

$$K_I = Ya^{1/2}\sigma \quad (1)$$

where a is the initial flaw length, and σ is the overall stress far from the crack. The factor Y is a function of (a/w) which is specified by the specimen geometry being used, where w is the specimen width. The Bowie[17] geometric factor for a double-edge-notch specimen (as in *Figure 1*) is utilized, where:

$$Y = 1.98 + 0.36(2a/w) - 2.12(2a/w)^2 + 3.42(2a/w)^3 \quad (2)$$

Sharp-notched specimens in conjunction with the fracture mechanics approach, provide a reasonable amount of experimental geometry independence with regard to crack length and specimen width, as well as providing a convenient flaw at which to observe crack nucleation and growth kinetics. The fracture mechanics approach also allows us to stipulate a precisely-defined initial polyaxial stress state. A constant strain test, such as the Bell[1,15] bent strip *ESC* test, will generally bias in favour of materials with lower Young's modulus within a given

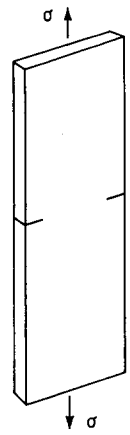

Figure 1 Double-edge-notched test specimen 95 x 13 x 3.2 mm with 1.3 mm deep razor slits. Slit length (a) and specimen width (w)

0032-3861/81/050682-05$02.00

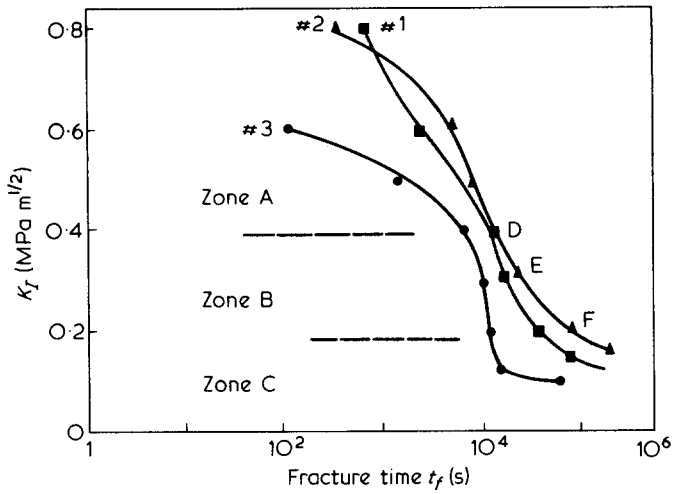

Figure 2 Initial stress intensity parameter K_I *versus* fracture time t_f for samples no. 1 (ρ = 0.962); no. 2 (ρ = 0.954); and no. 3 (ρ = 0.935). Melt index range of 4.0 to 5.0

polymer type. As will be shown, *ESC* resistance does not necessarily coincide with decreasing modulus.

Rectangular specimens were prepared from flat pieces of polyethylene, which can be fabricated by compression or injection moulding, and/or any particular orientation state that we wish to study. The specimens were machined to the dimensions shown with 1.3 mm deep razor slits cut into the samples. Specimens can be cut so that the slits are parallel or perpendicular to the orientation directions. The specimens were each fitted with a sealed cylindrical fixture for containment of the aggressive liquid environments (10% Igepal CO–630 and 90% H_2O for any data presented here). Grips were attached to both ends of the specimen. The specimens were then hung in a hot air tank at 50°C. Upon reaching the required temperature (usually in about 10 min), a group of specimens were subjected to a range of loads. Fracture of the specimens was noted by automatic shut-off timers; thus yielding the initial stress intensity factor K_I (MPa·m$^{1/2}$) *versus* fracture time, t_f, data (log t_f is plotted, as shown in *Figure 2*). Special care was taken both to cut razor slits of equal length, and to obtain exact alignment of the specimen grips. These steps are necessary to ensure that the environmental stress cracks associated with the two slits start and grow together. Because of the test specimen configuration, one can readily study the kinetics of environmental stress cracking by time lapse photography.

In an effort to relate *ESCR* properties of polyethylenes to their microstructures, bulk structure characterization was carried out by a combination of transmission electron microscopy (*TEM*), scanning transmission electronic microscopy (*STEM*), small-angle X-ray scattering (SAXS), and small-angle light scattering (SALS). In addition, some fracture surfaces were examined by scanning electron microscopy (*SEM*).

HDPE specimens for electronic microscopy were prepared by treatment with chlorosulphonic acid which creates activated sites in the amorphous regions to attract uranium atoms for the selective staining with uranyl acetate. After staining, the specimens were ultramicrotomed in a cold stage. The uranium is more opaque to electron beam transmission and, consequently, the amorphous regions appear as dark areas in an electron microscope image. *SEM* was performed on HDPE fracture surfaces which had gold vapour deposited on them. The viewing angle used was 20°. SAXS and SALS were, respectively, utilized to measure micropore content and spherulite size by photographic film techniques outlined by Samuels[9].

Compression-moulded PE samples were fabricated from 3.2 mm thick sheet moulded with a long and moderate cooling cycle. Injection moulded specimens were prepared by first moulding 95 x 13 x 3.2 mm plaques as shown in *Figure 3* in a New Britain injection moulding machine. Because the plaque mould is a flow-through design with quench occurring during viscous flow, orientation increases as the plaque is transversed from the gate side to the vent side of the mould.

RESULTS AND DISCUSSION

Curves of initial K_I *versus* log t_f data for sample no. 1 (a homopolymer, $\rho = 0.962$ and melt index $MI = 5.0$) and propylene copolymer samples no. 2 ($\rho = 0.954$, $MI = 4.0$) and no. 3 ($\rho = 0.935$, $MI = 5.0$) are presented in *Figure 2*. The data curves have a sigmoidal shape over a K_I range of 1 MPa m$^{1/2}$. The times to fracture at the lower K_I values in the 'knee' of the curve actually consist of an incubation time t_d and the crack growth, as shown by the crack length l *versus* $t^{1/2}$ plots in *Figure 4*. The data indicates that the environmental stress crack resistance (*ESCR*) is maximized at the middle density ($\rho = 0.954$) of specimen no. 2 and that the principle difference between the resins is t_d and *not* the crack growth rate. The incubation times t_d and average crack velocities $\bar{v}$ are: sample no. 1, $t_d = 10\,200$ s and $\bar{v} = 1.6 \times 10^{-5}$ cm s^{-1}; sample no. 2, $t_d = 27\,000$ s and $\bar{v} = 1.6 \times 10^{-5}$ cm s^{-1}; and sample no. 3, $t_d = 4000$ s and $\bar{v}$ pendent than the values of $\bar{v}$, and t_d thus becomes similar in kind to what has also been observed by

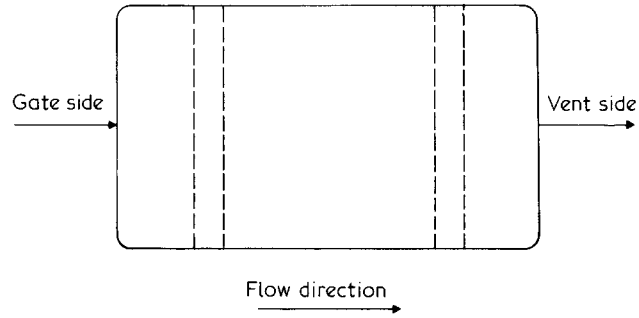

Figure 3 10.2 x 17.8 cm injection moulded plaque with transversely cut specimens

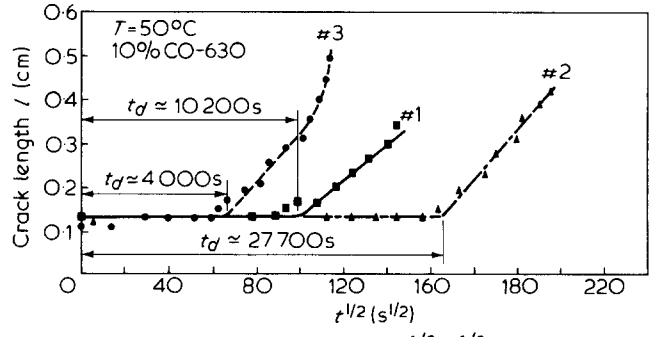

Figure 4 Crack length l *versus* root time $t^{1/2}$ (s$^{1/2}$) for samples no. 1, no. 2, and no. 3. Initial K_I = 0.2 MPa m$^{1/2}$

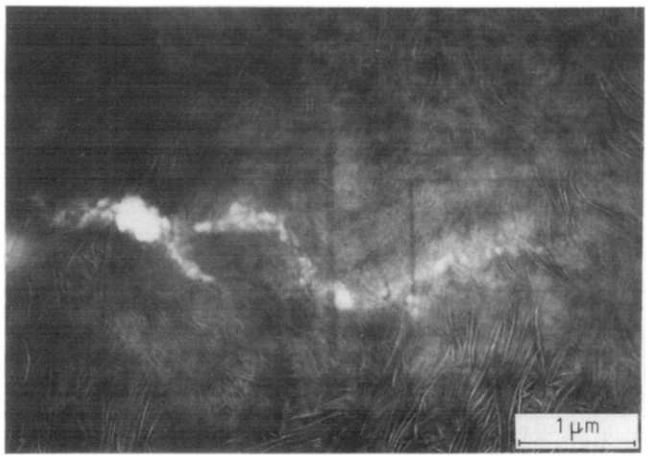

Figure 5 Bright field transmission electron photomicrograph of a dry craze ahead of a mature environmental stress crack in an intermediate density PE

Crissman and Zapas[18] for *ESC* failure of pressurized PE diaphrams in contact with detergent.

The sigmoidal curves of *Figure 2* can be divided into three zones (A, B and C) denoting different fracture processes. Zone A is the stress dependent region predominantly of dry creep rupture. Zone B, with greater stress independence, is the region where transport of aggressive liquid through a pore/fibril structure at the crack tip strongly controls the crack growth rate. Capillary force is presumably the driving force for the liquid transport, similar in kind to that which has been demonstrated for solvent crazing in glass polymers[8,11]. More evidence will subsequently be presented to support this hypothesis. Zone C returns to an increased stress dependence because a large portion of the fracture time is attributed to the incubation time for cracking (t_d). In cubation times for polymer deformation are stress dependent in a fashion analogous to the Eyring[10] theory of rate processes. For example, at points D, E and F of sample no. 2 in *Figure 2*, we obtain using time-lapse photography data:

Sample no. 2, ρ = 0.954, *MI* = 4.0

	K_I (MPa m$^{1/2}$)	t_d (s)	$\bar{v}_c$ (cm s^{-1})
(D)	0.4	1100	2.3×10^{-5}
(E)	0.3	10000	2.0×10^{-5}
(F)	0.2	27700	1.6×10^{-5}

The incubation times are considerably more stress dependent than the values of $\bar{v}$, and t_d thus becomes progressively less significant with respect to t_f as zone C is entered. Incubation times for *ESC* of low density PE and low molecular weight HDPE have also been observed by Bandyopadhyay and Brown[19].

t_d is the time required to form sufficient dry crazes and voids to allow the PE to absorb the aggressive liquid. The dry void formation zone can often be seen with the naked eye and is approximately 1 mm long. *Figure 5* shows a transmission electron photomicrograph of a craze front of a mature environmental stress crack in an intermediate density polyethylene. It should be emphasized that the ultramicrotome section was obtained from a dry section of material ahead of the liquid front in the void region at the crack tip. The craze appears to be branched, and examination of the craze tip by *TEM* (*Figure 6*) shows the alternating void–fibril arrangement similar to that found for crazes in glassy polymers[20]. The void diameter appears to be typically ~300 Å. This evidence leaves little doubt that an environmental stress crack in PE is preceded by a dry craze.

The $t^{1/2}$ dependent crack growth kinetics can be explained with the aid of the *SEM* photomicrograph in *Figure 7*. Looking along the axis of the crack towards the tip, it can be seen that the crack tunnels through the material by forming a lip around the crack tip and crack sides towards the tip. Similar tunnelling has been observed by Marshall *et al.*[5]. This restricted side flow, where fluid flow is allowed only up the axis of this crack, has been demonstrated to determine t^n ($n < 1$) craze or crack growth in polymers[5,6,8,11]. The tip of the crack with its fibril and void structure can be modelled as a fluid flow problem perpendicular to an hexagonal array of cylindrical rods with their axes oriented perpendicular to the crack plane, in a fashion similar to that attempted for solvent crazing by Kramer and Bubeck[8,11]. According to the model, the exponent $n = 1/2$ for $t^{1/2}$ kinetics is a result of a fibril

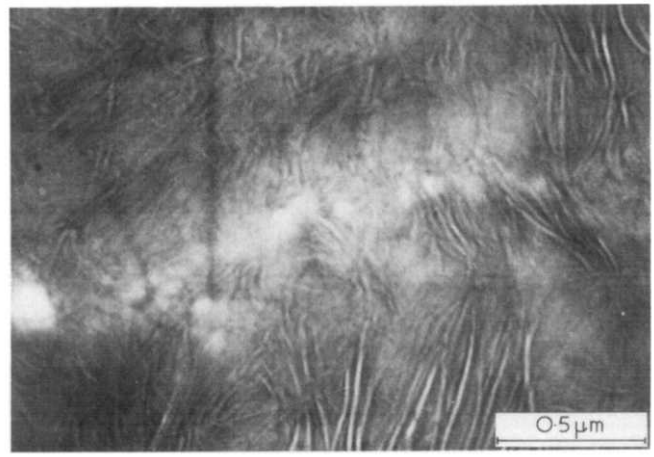

Figure 6 High magnification electron photomicrograph of the tip of the craze shown in *Figure 5*

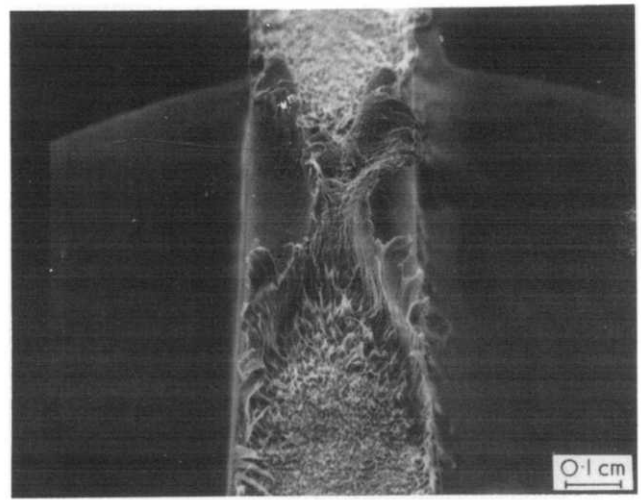

Figure 7 Scanning electron photomicrograph of fracture surface close to environmental stress crack tip showing the tunnelling effect. Vertical axis of micrograph is parallel to direction of crack growth

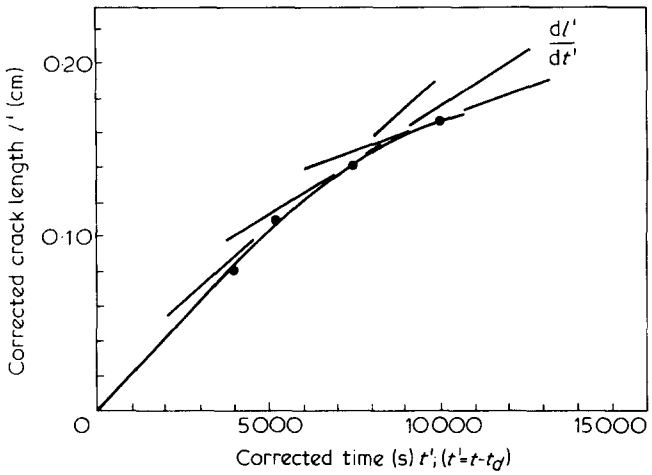

Figure 8 Corrected crack length l' *versus* corrected time t' for sample no. 1

volume fraction V_f distribution at the craze/crack tip for the restricted side flow case. If the protective lip was not present, there would be unrestricted side flow for which the transport distance would be a constant equal to one-half the specimen thickness, yielding t ($n=1$) dependence.

Using the transport control model[11], if the crack growth velocity is limited by the fluid velocity through the pore structure, then:

$$\frac{1}{l'}\left(\frac{P_c+P_a}{\mu\langle(1-V_f)/k'\rangle}\right)=\frac{dl'}{dt'} \tag{3}$$

where l' is the corrected crack length $l-a$, t' is the corrected time where $t'=t-t_d$, P_c is capillary pressure, P_a atmospheric pressure, V_f is the fibril volume fraction at l', and k' is Darcy's constant for the fibrillar array, where:

$$k'=\frac{D^2}{32V_f}\left[\ln\left\{\frac{1}{V_f}\right\}-\frac{1-V_f^2}{1+V_f^2}\right] \tag{4}$$

Equation (4) is the Happel[16] solution to flow perpendicular to a solid cylinder where D is the cylinder (i.e. fibril) diameter. A typical plot of l' *versus* t' is shown in *Figure 8* for sample no. 1 where it can be seen that over a range of l of 0.2 cm the instantaneous crack velocity is decreasing with time. Using equation (3) the crack growth data from *Figure 4* should yield a straight line with an intercept at the origin. This indeed occurs, with good agreement, for samples no. 1 and no. 2 in *Figure 9* ($l' \geqslant 0.08$ cm).

Both Marshall *et al.*[5] and Bandyopadhyay[19] do not observe a $t^{1/2}$ dependence in crack growth velocity, but rather measure a steadily accelerating velocity, as determined with single-edge-notched specimens. This discrepancy can possible be explained by noting the differences in test specimens utilized and the relatively poor creep resistance of polyethylene, particularly low density polyethylene, in general. *ESC* testing by this author of single-edge-notched specimens of 15 to 30 mm in width show perceptable hinging during crack growth and increasing instantaneous K_I, particularly at 50°C. *ESC* testing with well-aligned double-edge-notch specimens results in an accelerating crack growth until the protective side lips are sufficiently formed to sustain approximate $t^{1/2}$ growth. As the growing cracks decrease the effective cross-section of the specimen, the remaining PE begins to creep rapidly, which results in a reaccelerating crack velocity. The l *versus* $t^{1/2}$ data in *Figure 4* for sample no. 3 (an intermediate density PE) shows the transition from $t^{1/2}$ dependence to accelerating crack growth at a crack length of approximately 0.35 cm in a 13 mm wide specimen. Before the onset of the contribution of creep to specimen failure, a $t^{1/4}$ dependent crack growth region has been observed in PE samples with a density as low as 0.925 g cm^{-3} at $K_I=0.2$ MPa m$^{1/2}$ and $T=50$°C using well-aligned double-edge-notched specimens.

A reported characteristic of an aggressive liquid agent for PE is that increased surface wetting promotes *ESC*[1,12]. The degree and rate of *ESC* appear to decrease with increased liquid viscosity[1,13]. The viscosity approach is also amply demonstrated for *ESC* in several polymer systems by the cracking kinetics studies of Williams and Marshall[6]. If one accepts the view that capillary pressure is the driving force for the cracking process, then surface tension and viscosity can be resolved as part of the same physical phenomenon.

Considering the hydrodynamic radius b around a fibril of radius a, the fibril volume fraction V_f is $(a/b)^2$. Using Equation (4), we obtain Darcy's constant $k' \simeq 1.3\times10^{-14}$ cm^2, where $a=150$ Å and $b=300$ Å are estimated from electron photomicrographs. Using equation (3) and the value for the slope $(l'dl'/dt')=1.3\times10^{-6}$ cm^2 s^{-1} from *Figure 9*, and using the measured value for the viscosity, μ, of 10% CO–630 solution ($\mu \simeq 0.3$ g cm^{-1} s^{-1} [14]) we can estimate $P_c \simeq 14$ atm. Next, the influence on P_c of a surface tension γ_{LV} can be estimated by Laplace's equation, as suggested by Kambour[20], viz,

$$P_c=\frac{\gamma_{LV}}{r}\cos\theta \tag{5}$$

With γ_{LV} (10% CO–630) ~ 37 dyne cm^{-1} (ref 1), $\cos\theta \simeq 1$ and $r=b=300$ Å, then $P_c \simeq 12$ atm. An estimated value of ~14 atm is thus obtained by both calculations for the capillary pressure controlling crack growth in the craze at the crack tip. (This estimate of P_c supersedes the preliminary estimate given elsewhere[21].)

The intermediate density PE, sample no. 3, propylene copolymer resin has poorer *ESC* resistance than the high density PE, sample no. 2. *Figure 4* indicates that the difference is primarily due to the incubation times, rather than the crack growth rates. Preliminary electron microscopy does indicate thay dry crazing and voiding occurs more readily in sample no. 3 (a future paper will discuss the influence of microstructure on incubation time and

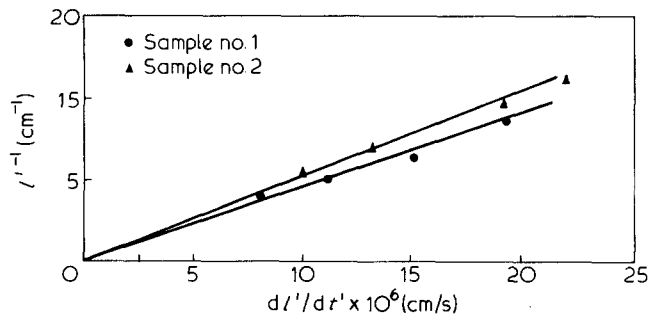

Figure 9 Reciprocal of corrected crack length l' *versus* the instantaneous crack growth velocity dl'/dt' showing agreement with equation (3)

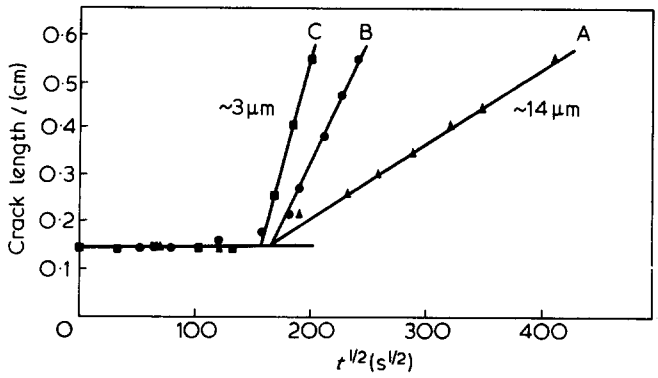

Figure 10 Crack length *l versus* root time $t^{1/2}$ for sample no. 4; A, compression moulded; B, injection moulded, moderate orientation; and C, injection moulded, high orientation. K_I = 0.2 MPa $m^{1/2}$. Average spherulite sizes are 14 μm for A and approximately 3 μm for B and C. ▲, No. 4 compression moulded; ●, no. 4 gate side; ■, no. 4 vent side

ESC). This case is an example of how a bent form constant strain test such as the Bell Laboratories test[15] which favours low modulus PE resins will obscure the true mechanism of *ESC* failure in a polymer. The copolymer sample no. 2 has superior *ESC* to that of sample no. 1, because the copolymerization favours the formation of intercrystalline links and tie molecules, which, as discussed by Peterlin[22,23], cause the microfibrils in PE crazes to be stronger.

The incubation time t_d and crack growth data for an HDPE resin sample no. 4 ($\rho = 0.954$, $MI = 6.0$) at $K_I = 0.2$ MPa $m^{1/2}$ for two injection moulded conditions (B and C) and for the compression moulded condition (A) are shown in *Figure 10*. Conditions B and C test strips were cut out of the injection moulded plaque at the gate and vent sides, respectively, as shown in *Figure 3*. For specimens tested for crack growth parallel to the direction of moulding orientation the crack growth rate increases with increasing orientation. The t_d, however, is independent of orientation. SALS measurements indicate that the compression moulded case for sample no. 4 has an average spherulite size of 14 μm and the injection moulded specimens average at 3 μm. By SAXS, the most severe injection moulded orientation has the highest initial micropore content. The incurring of smaller spherulite size and higher initial micropore content by injection moulding apparently affects primarily the fibrillation process during crack growth. Increasing the number of defects in a semicrystalline polymer interferes with the microfibrillization during cold drawing, according to Peterlin[22,23]. The increased number of defects caused by injection moulding, as manifested by smaller spherulite size and greater micropore content, apparently result in crazes with a decreased fibril volume fraction that are more conducive to aggressive liquid flow.

ACKNOWLEDGEMENTS

Thanks are extended to C. S. P. Sung of MIT for the SAXS and SALS measurements reported here. Special thanks are due to H. Baker of Dow Chemical for the electron microscopy specimen preparation. Useful discussions with F. J. McGarry (also of MIT) are gratefully acknowledged.

REFERENCES

1 Howard, J. B. Ch. 11 of 'Engineering Design for Plastics' (Ed. E. Baer) Rheinhold, New York, 1964, pp 742–794
2 Gaube, E. *Kunstoffe* 1959, **49**, 446
3 Frayer, P. D., Tong, P. P. and Dreher, W. W. *Polym. Eng. Sci.* 1977, **17**, 1, 27
4 Soni, P. and Geil, P. M. Dept. of Macromolecular Science Report TR No. 286, Case Western Reserve University (Sept. 1975)
5 Marshall, G. P., Linkins, M. M., Culver, L. E. and Williams, J. G. *SPE J.* 1972, **28**, 26
6 Williams, J. G. and Marshall, G. P. *Proc. Roy. Soc. London (A)* 1975, **342**, 55
7 Hayes, D. J. *J. Strain Anal.* 1975, **10**, 4, 198
8 Bubeck, R. A. *PhD Thesis*, Cornell University, (1976)
9 Samuels, R. J. 'Structural Polymer Properties', Wiley, New York, 1974, pp 74–103
10 Eyring, H. E. *J. Chem. Phys.* 1936, **4**, 283
11 Kramer, E. J. and Bubeck, R. A. *J. Polym. Sci. (Polym. Phys. Edn)* 1978, **16**, 1195
12 Shanahan, M. E. R., Schultz, J. *J. Polym. Sci. (Polym. Phys. Edn)* 1978, **16**, 863
13 Schultz, J. and Shanahan, M. E. R. *Polym. Prepr.* 1977, **18**, 2
14 Viscosity measurement of 10% CO–630 solution used for this study at 50°C. According to ref 1, the viscosity should be between approximately 0.1 and 0.75 g cm^{-1} s^{-1}
15 ASTM Designation D1693–66: 'Standard method of test for environmental stress-cracking of type I ethylene plastics', 1971. Annual Book of ASTM Standards, Part 26, American Society for Testing and Materials, Philadelphia, 1971
16 Happel, J. and Brenner, H. 'Low Reynolds Number Hydrodynamics', Prentice Hall, Englewood Cliffs, New Jersey, 1965, 395
17 Brown, W. F. and Srawley, J. E. 'Plane Strain Crack Toughness Testing for High Strength Metallic Materials', *ASTM STP 410*, American Society for Testing and Materials, Philadelphia, 1966, 11
18 Crissman, J. M. and Zapas, L. J. *ASC Organic Coatings and Plastics Chemistry Preprints* 1979, **41**, 475
19 Bandyopadhyay, F. *PhD Thesis*, Monash University, Melbourne, Australia (1979)
20 Kambour, R. P. *J. Polym. Sci. Macromol. Rev.* 1973, **7**, 1
21 Bubeck, R. A. *ASC Organic Coatings and Plastics Chemistry Preprints* 1979, **41**, 481
22 Peterlin, A. in 'Polymeric Materials' (Eds. E. Baer and S. V. Radcliffe) The American Society for Metals, 1975, pp 203–234
23 Peterlin, A. *ASC Organic Coatings and Plastics Chemistry Preprints* 1979, **41**, 399